Acoustic levitation in the presence of gravity

P. Collas
Department of Physics and Astronomy, California State University, Northridge, California 91330

M. Barmatz and C. Shipley
Jet Propulsion Laboratory, California Institute of Technology, Pasadena, California 91109

(Received 27 September 1988; accepted for publication 21 April 1989)

The method of Gor'kov has been applied to derive general expressions for the total potential and force on a small spherical object in a resonant chamber in the presence of both acoustic and gravitational force fields. The levitation position is also determined in rectangular resonators for the simultaneous excitation of up to three acoustic modes, and the results are applied to the triple-axis acoustic levitator. The analysis is applied to rectangular, spherical, and cylindrical single-mode levitators that are arbitrarily oriented relative to the gravitational force field. Criteria are determined for isotropic force fields in rectangular and cylindrical resonators. It is demonstrated that an object will be situated within a volume of possible levitation positions at a point determined by the relative strength of the acoustic and gravitational fields and the orientation of the chamber relative to gravity. Trajectories of an object from an arbitrary starting position to a final equilibrium position are also discussed.

PACS numbers: 43.25.Qp, 43.25.Uv, 43.25.Gf

INTRODUCTION

Acoustic forces can be used to position and manipulate materials.[1] NASA is now developing acoustic positioning techniques for processing materials in the microgravity environment of space.[1,2] In preparation for future space research, considerable development work on acoustic levitators is now being carried out in ground-based laboratories where both gravitational and acoustic forces are present. King[3] was the first to develop a detailed analysis of the acoustic force on an incompressible sphere. Yosioka and Kawasima[4] extended King's work to include a compressible sphere. The early theoretical and experimental work of Crum[5] demonstrated the viability of using acoustic and gravitational fields to accurately position droplets in a fluid. This method was subsequently employed to measure physical properties of suspended samples.[6] In a previous paper,[7] we applied Gor'kov's acoustic potential method[8] for deriving forces on a particle in an arbitrary acoustic field to the case of standing waves in rectangular, spherical, and cylindrical resonators. Gor'kov's theory was used to determine which classes of acoustic modes would uniquely position a sample in the interior of the resonator. We have also extended Gor'kov's theory to include the effects of a temperature gradient within the resonant cavity.[9]

In the present paper, we extend the previous work to include the effects of a gravitational field. In Sec. I, expressions are derived for the total potential and forces for the excitation of acoustic modes in rectangular, spherical, and cylindrical geometries that are arbitrarily oriented relative to gravity. The stable levitation positions within the chamber correspond to particular minima of the total potential. In Sec. II, the analysis is expanded to include the simultaneous excitation of several acoustic modes. An important application of the levitation technique is the triple-axis levitator[10] where three orthogonal plane-wave fields are simultaneously excited in a rectangular chamber to uniquely position a sample. By using degenerate orthogonal modes, this method can also develop acoustic torques to rotate the sample.[11]

In general, the acoustic force field associated with a single acoustic mode is anisotropic. Thus the shape of a positioned liquid sample will be nonspherical in the presence of only one acoustic mode in a zero-g environment. However, by including an external force, one can adjust the experimental parameters to control the isotropy of the total force field. In Sec. III, we have determined the necessary experimental conditions to produce an isotropic total force field at the position of a levitated sample for selected modes in rectangular and cylindrical chambers. In Sec. IV, the resulting expressions for the total potential in various geometries are applied to acoustic modes that are ideally suited for levitation purposes in order to determine the sample levitation position and maximum restoring forces. Concluding remarks are given in Sec. V.

I. THEORY

A. Definitions and notation

We shall adopt the following notation for all geometries. The total radiation potential U of an acoustic system in gravity is the sum of the acoustic potential U_a and the gravitational potential U_g:

$$U = U_a + U_g, \tag{1}$$

where

$$U_g = (m_s - m_f)gh = F_g h, \tag{2}$$

and m_s is the mass of the sample, m_f is the mass of the fluid displaced by the sample, and F_g is the total gravitational force. In all cases, the function h depends on the geometric coordinates and the angles that specify the orientation of the chamber.

The total force components are obtained from the gradi-

 0001-4966/89/080777-11$00.80

ent of the potential $\mathbf{F} = -\text{grad}\, U$. We let

$$F_i = F_{ai} + F_{gi}, \tag{3}$$

where F_{ai} are the acoustic force components, $F_{gi} = F_g w_i$ are the projected gravitational terms, and F_i are the resulting total force components. The subscript i stands for (x,y,z), (r,θ,ϕ), and (r,ϕ,z) in the rectangular, spherical, and cylindrical case, respectively. The $w_i = \partial h/\partial x_i$ are gravitational projection functions that depend on the angular coordinates and the orientation angles.

For convenience, we define the following dimensionless quantities adopting the normalization of Ref. 7:

$$\tilde{p} = p_{in}/(\rho_f c v_o), \quad \tilde{v} = v_{in}/v_o, \tag{4}$$

$$\tilde{U} = U/(\pi R^3 \rho_f v_o^2), \quad \tilde{U}_a = U_a/(\pi R^3 \rho_f v_o^2), \tag{5}$$

$$\tilde{F}_i = F_i/(\pi R^3 \rho_f v_o^2 k), \quad \tilde{F}_{ai} = F_{ai}/(\pi R^3 \rho_f v_o^2 k), \tag{6}$$

where $k = w/c$ and v_o is the particle velocity parameter; i.e., $\mathbf{v} = (v_o/k)\text{grad}\,\tilde{\Phi}_{in}$ with $\tilde{\Phi}_{in}$ a normal mode of the chamber.[12] The acoustic pressure $\tilde{p}_{in}$, particle velocity $\tilde{v}_{in}$, and potential $\tilde{U}_a$ are given in Ref. 7 for rectangular, spherical, and cylindrical geometries discussed in this paper. The density and sound velocity in the surrounding fluid are given by ρ_f and c, respectively. We also introduce a normalized gravitational force given by

$$\tilde{F}_g = F_g/(\pi R^3 \rho_f v_o^2 k) = 4(\rho_s - \rho_f)g/(3\rho_f v_o^2 k), \tag{7}$$

where ρ_s is the density of the spherical sample.

In Ref. 7, we found it useful to introduce the concept of effective restoring force constants κ_i as a measure of the stability provided by the potential well in the various directions. These constants are equal to eigenvalues of the Hessian matrix, which consists of the second partial derivatives of U with respect to the spatial coordinates, *evaluated at the location of the minimum of the potential.* The normalized dimensionless restoring force constants are defined by

$$\tilde{\kappa}_i = \frac{\partial^2 \tilde{U}}{\partial \tilde{x}_i^2}, \tag{8}$$

where, in rectangular geometry, the spatial coordinates x_i are $\tilde{x} = kx''$, $\tilde{y} = ky''$, and $\tilde{z} = kz''$, in spherical geometry, $\tilde{r} = k_{ln} r''$, $\tilde{\theta} = \tilde{r}\theta''$, and $\tilde{\phi} = \tilde{r}\sin\theta\phi''$, and, in cylindrical geometry, $\tilde{r} = k_c r''$, $\tilde{\phi} = \tilde{r}\phi''$, and $\tilde{z} = k_c z''$. The double prime coordinates refer to the system that diagonalizes the Hessian. The wavenumbers are given by

$$k = (k_x^2 + k_y^2 + k_z^2)^{1/2},$$

with

$$k_x = \frac{\pi n_x}{l_x}, \quad k_y = \frac{\pi n_y}{l_y}, \quad k_z = \frac{\pi n_z}{l_z},$$

where the n's and l's are mode numbers $(n_x n_y n_z)$ and chamber dimensions, respectively, and

$$k_{ln} = \frac{\pi \gamma_{ln}}{r_o},$$

where r_o is the spherical chamber radius and γ_{ln} is a solution of $d[j_l(\pi\gamma)]/d\gamma = 0$ with j_l being the spherical Bessel function of order l and

$$k_c = (k_r^2 + k_z^2)^{1/2},$$

with

$$k_r = \pi\alpha_{mn}/a,$$

where a is the cylindrical radius and α_{mn} is a solution of $d[J_m(\pi\alpha)]/d\alpha = 0$, with J_m being the Bessel function of order m. As we shall see, the gravitational potential $\tilde{U}_g$ is linear in the $\tilde{x}_i$, and, consequently, the critical points of $\tilde{U}$ will be spatially shifted relative to the critical points of $\tilde{U}_a$, however, their type[7] will remain unchanged since $\partial^2\tilde{U}/\partial\tilde{x}_i^2 = \partial^2\tilde{U}_a/\partial\tilde{x}_i^2$, etc. In particular, the minima of $\tilde{U}$ will correspond to the shifted minima of $\tilde{U}_a$. The direction of the shift will, of course, depend on the orientation of the chamber. As the minima of $\tilde{U}$ are shifted by gravitation, the restoring force constants will correspondingly change.

B. Rectangular geometry

For rectangular geometry, the gravitational projection functions w_i used in Eq. (3) are simply the direction cosines; thus

$$w_x = \lambda = \cos\alpha, \quad w_y = \mu = \cos\beta, \quad w_z = \nu = \cos\gamma, \tag{9}$$

where $\lambda^2 + \mu^2 + \nu^2 = 1$ (see Fig. 1). The normalized potential now becomes

$$\tilde{U} = \tilde{U}_a - \tilde{F}_g k(\lambda x + \mu y + \nu z), \tag{10}$$

where $\tilde{U}_a$ is given by[7]

$$\tilde{U}_a = \frac{f_1}{3}\cos^2 k_x x \cos^2 k_y y \cos^2 k_z z - \frac{f_2}{2}\left[\left(\frac{k_x}{k}\right)^2 \sin^2 k_x x \times \cos^2 k_y y \cos^2 k_z z + \left(\frac{k_y}{k}\right)^2 \cos^2 k_x x \sin^2 k_y y \times \cos^2 k_z z + \left(\frac{k_z}{k}\right)^2 \cos^2 k_x x \cos^2 k_y y \sin^2 k_z z\right]. \tag{11}$$

The factors f_1 and f_2 are given by $f_1 = 1 - \rho_f c^2/\rho_s c_s^2, f_2 = 2(\rho_s - \rho_f)/(2\rho_s + \rho_f)$, where c_s is the sound velocity in the spherical sample. The term $\tilde{F}_g k(\lambda x + \mu y + \nu z)$, in Eq. (10), vanishes on a plane that is perpendicular to $\mathbf{F}_g$ and passes through the origin.

The force components are given by

$$\tilde{F}_i = \tilde{F}_{ai} + \tilde{F}_g w_i, \tag{12}$$

where

$$\mathbf{w} = w_i \mathbf{e}_i = \lambda \mathbf{e}_x + \mu \mathbf{e}_y + \nu \mathbf{e}_z. \tag{13}$$

For example,

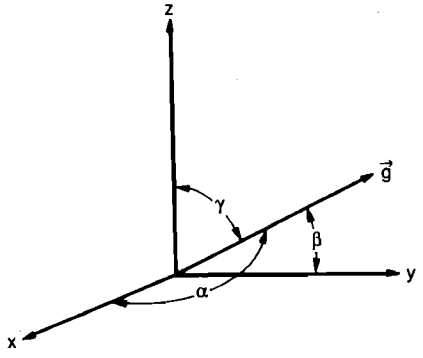

FIG. 1. Orientation of gravity in rectangular geometry; α, β, and γ are the angles the gravity vector makes with the x, y, and z axis, respectively.

$$\tilde{F}_{ax} = \left(\frac{k_x}{k}\right)\sin 2k_x x\left\{\left[\frac{f_1}{3} + \left(\frac{f_2}{2}\right)\left(\frac{k_x}{k}\right)^2\right]\cos^2 k_y y \times \cos^2 k_z z - \left(\frac{f_2}{2}\right)\left[\left(\frac{k_y}{k}\right)^2 \sin^2 k_y y \cos^2 k_z z + \left(\frac{k_z}{k}\right)^2 \cos^2 k_y y \sin^2 k_z z\right]\right\}. \quad (14)$$

To obtain $\tilde{F}_{ay}$ and $\tilde{F}_{az}$, simply interchange $x \leftrightarrow y$ and $x \leftrightarrow z$, respectively, in Eq. (14).

C. Spherical geometry

By choosing $\tilde{U} = 0$ on a plane through the origin and perpendicular to $\mathbf{F}_g$ we have

$$\tilde{U} = \tilde{U}_a - \tilde{F}_g k_{ln} r \cos\gamma, \quad (15)$$

where γ is the angle between the gravitational direction (θ',ϕ') and any other direction (θ,ϕ), as shown in Fig. 2. From geometrical considerations, it follows that

$$\cos\gamma = \cos\theta\cos\theta' + \sin\theta\sin\theta'\cos(\phi - \phi'). \quad (16)$$

The dimensionless acoustic potential $\tilde{U}_a$ is given by[7]

$$\tilde{U}_a = \left(\frac{f_1}{3}\right) j_l^2(\zeta)\,[P_l^m(\mu)]^2\cos^2 m\phi - \left(\frac{f_2}{2}\right) \times \left\{\left(\frac{l j_l(\zeta)}{\zeta} - j_{l+1}(\zeta)\right)^2 [P_l^m(\mu)]^2\cos^2 m\phi + \left[\left(\frac{j_l(\zeta)}{\zeta}\right)^2 \Big/ (1-\mu^2)\right]\{[(l+1)\mu P_l^m(\mu) - (l-m+1)P_{l+1}^m(\mu)]^2\cos^2 m\phi + [mP_l^m(\mu)]^2\sin^2 m\phi\}\right\}, \quad (17)$$

where $\zeta = \tilde{r} = k_{ln} r$ and $\mu = \cos\theta$.

The gravitational contributions to the force components are given by $\tilde{F}_g k\mathbf{w}$, where

$$\mathbf{w} = w_i \mathbf{e}_i = \cos\gamma\,\mathbf{e}_r + [-\sin\theta\cos\theta' + \cos\theta\sin\theta'\cos(\phi - \phi')]\mathbf{e}_\theta - \sin\theta'\sin(\phi - \phi')\mathbf{e}_\phi. \quad (18)$$

The corresponding expressions for the F_{ai} are rather involved and can be found in Appendix C of Ref. 7.

D. Cylindrical geometry

Here, we let the sphere of the previous section be enclosed by a cylinder, so that the polar axis of the sphere coincides with the z axis of the cylinder (see Fig. 3). We then have

$$r_s = \sqrt{z^2 + r^2}, \quad \cos\theta = z/r_s = z/\sqrt{z^2 + r^2}, \quad \sin\theta = r/r_s = r/\sqrt{z^2 + r^2}, \quad (19)$$

where r and r_s are the cylindrical and spherical radial coordinates, respectively. Substituting Eqs. (19) into Eq. (16), we obtain

$$\cos\gamma = [z\cos\theta' + r\sin\theta'\cos(\phi - \phi')]/\sqrt{z^2 + r^2}, \quad (20)$$

while Eq. (15) becomes

$$\tilde{U} = \tilde{U}_a - \tilde{F}_g k_c r_s \cos\gamma = \tilde{U}_a - \tilde{F}_g k_c [z\cos\theta' + r\sin\theta'\cos(\phi - \phi')]. \quad (21)$$

Here, $\tilde{U}_a$ is given by[7]

$$\tilde{U}_a = \left(\frac{f_1}{3}\right) J_m^2(\chi)\cos^2 m\phi\cos^2 k_z z - \left(\frac{f_2}{2}\right)\left\{\left(\frac{k_r}{k}\right)^2 \times \left[\left(\frac{mJ_m(\chi)}{\chi}\right)^2 - J_{m+1}(\chi) \times \left(\frac{2mJ_m(\chi)}{\chi} - J_{m+1}(\chi)\right) \times \cos^2 m\phi\right]\cos^2 k_z z + \left(\frac{k_z}{k}\right)^2 \cos^2 m\phi\sin^2 k_z z\right\}, \quad (22)$$

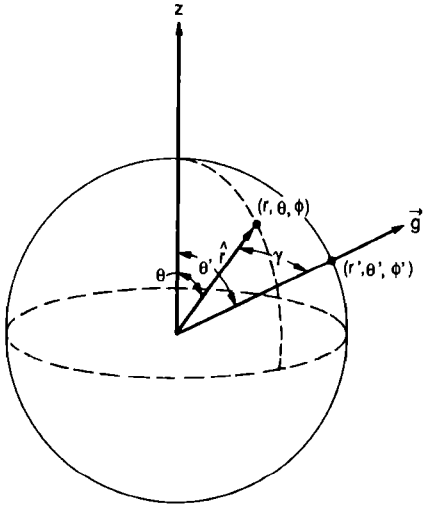

FIG. 2. Orientation of gravity in spherical geometry. The angles θ', ϕ' are the spherical azimuthal and polar angles that define the gravity direction. The origin of the angles θ', ϕ' depends on the mode of excitation.

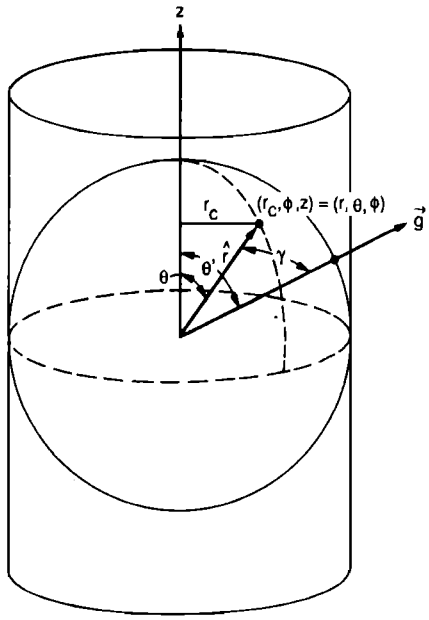

FIG. 3. Orientation of gravity in cylindrical geometry. The gravity direction is defined by the spherical azimuthal and polar angles θ' and ϕ'. The azimuthal angle θ' is referenced to the z axis while the polar angle origin depends on the mode of excitation.

where $\chi = k_r r$.

Note that we have again chosen the gravitational potential to vanish on a plane through $z = 0$ and perpendicular to $\mathbf{F}_g$. The gravitational contributions to the force components are given by $\tilde{F}_g k\mathbf{w}$, where now

$$\mathbf{w} = w_i \mathbf{e}_i = \sin\theta' \cos(\phi - \phi')\mathbf{e}_r - \sin\theta' \sin(\phi - \phi')\mathbf{e}_\phi + \cos\theta' \mathbf{e}_z. \tag{23}$$

The corresponding expressions for the $\tilde{F}_{ai}$ may be found in Appendix C of Ref. 7.

II. SIMULTANEOUSLY EXCITED MODES

In the previous section, we discussed levitators in which only one excited mode was necessary to uniquely position an object. It is also possible to use several simultaneously excited modes to produce the same results. In certain cases, such as a triple-axis levitator, the application of many modes leads to sample manipulation as well as positioning capabilities.[1]

We will consider here the case where the sample is positioned in a resonator in the presence of three simultaneously excited modes. In this case, we have for the total pressure and particle velocity,

$$P_{in} = \sum_i P_i \quad \text{and} \quad \mathbf{V}_{in} = \sum_i \mathbf{V}_i = \sum_{ij} V_{ij}\mathbf{e}_j, \tag{24}$$

where the subscript i corresponds to the ith excited mode and the j corresponds to the three orthogonal directions for the given geometry. The total acoustic potential U_{Ta} is obtained by substituting P_{in} and $\mathbf{V}_{in}$ from Eq. (24) into Gor'kov's potential expression.[8] Possible degeneracies between two or more sound waves are taken into account by introducing a phase angle Δ in the time dependence.

For illustration purposes, we shall restrict ourselves to the rectangular geometry; however, the extension of this analysis to spherical or cylindrical geometry is straightforward. For a rectangular chamber, we have

$$P_i = p_i \sin(\omega_i t + \Delta_i) \quad \text{and} \quad V_{ij} = v_{ij} \cos(\omega_i t + \Delta_i), \tag{25}$$

where

$$p_i = -p_{io} \cos k_{ix}x \cos k_{iy}y \cos k_{iz}z = -p_{io}\tilde{p}_i, \tag{26}$$

and

$$\begin{aligned} v_{ix} &= (k_{ix}/k_i)v_{io} \sin k_{ix}x \cos k_{iy}y \cos k_{iz}z = v_{io}\tilde{v}_{ix}, \\ v_{iy} &= (k_{iy}/k_i)v_{io} \cos k_{ix}x \sin k_{iy}y \cos k_{iz}z = v_{io}\tilde{v}_{iy}, \\ v_{iz} &= (k_{iz}/k_i)v_{io} \cos k_{ix}x \cos k_{iy}y \sin k_{iz}z = v_{io}\tilde{v}_{iz}, \\ v_i^2 &= v_{ix}^2 + v_{iy}^2 + v_{iz}^2 = v_{io}^2\tilde{v}_i^2, \end{aligned} \tag{27}$$

where $k_i^2 = k_{ix}^2 + k_{iy}^2 + k_{iz}^2 = w_i^2/c^2$.

After carrying out the time averaging of the total pressure and velocity and using the relation $p_{io} = \rho_f c v_{io}$, we obtain for the total acoustic potential normalized to the first mode:

$$\tilde{U}_{Ta} = U_{Ta}/(\pi R^3 \rho_f v_{1o}^2) = \sum_{i=1}^{3} \tilde{U}_i + \sum_{i<j} \tilde{U}_{ij}\delta_{\omega_i\omega_j} \cos\Delta_{ij}, \tag{28a}$$

where

$$\tilde{U}_i = \left(\frac{p_{io}}{p_{1o}}\right)^2 \left(\frac{\tilde{p}_i^2 f_1}{3} - \frac{v_i^2 f_2}{2}\right) \tag{28b}$$

and

$$\tilde{U}_{ij} = (p_{io}p_{jo}/p_{1o}^2)[2\tilde{p}_i\tilde{p}_j f_1/3 - (v_{ix}v_{jx} + v_{iy}v_{jy} + v_{iz}v_{jz})f_2]. \tag{28c}$$

The phase difference $\Delta_{ij} = \Delta_i - \Delta_j$ and $\delta_{\omega_i\omega_j}$ is a Kronecker delta. The normalized potential $\tilde{U}_i$ and $\tilde{U}_{ij}$ have been written in terms of acoustic pressure ratios that can easily be obtained from experiment. There are three possible cases: The *nondegenerate case*, where $\omega_1 \neq \omega_2$, $\omega_1 \neq \omega_3$, $\omega_2 \neq \omega_3$; the *mixed case*, where, e.g., $\omega_1 = \omega_2$, but $\omega_1 \neq \omega_3$; and the *degenerate case*, where $\omega_1 = \omega_2 = \omega_3$.

The total potential is given by a relation formally identical to Eq. (10), viz.,

$$\tilde{U} = \tilde{U}_{Ta} - \tilde{F}_g k(\lambda x + \mu y + \nu z). \tag{29}$$

The gravitational terms in the force components are given by $\tilde{F}_g k\mathbf{w}$, with $\mathbf{w}$ given by Eq. (13), while the acoustic force components are given by $\tilde{F}_a = -\text{grad}\,\tilde{U}_{Ta}$.

The mixed case, which contains two degenerate modes, is the most interesting since it corresponds to the triple-axis levitator design now being used in space studies. For the (100), (010), (001) orthogonal set of plane wave modes, the total acoustic potential is given by

$$\begin{aligned} \tilde{U}_{Ta} = {} & \frac{f_1}{3}\left[\cos^2 k_1 x + \left(\frac{p_{2o}}{p_{1o}}\right)^2 \cos^2 k_1 y + \left(\frac{p_{3o}}{p_{1o}}\right)^2 \cos^2 k_3 z\right] \\ & - \frac{f_2}{2}\left[\sin^2 k_1 x + \left(\frac{p_{2o}}{p_{1o}}\right)^2 \sin^2 k_1 y + \left(\frac{p_{3o}}{p_{1o}}\right)^2 \sin^2 k_3 z\right] \\ & + (2f_1/3)(p_{2o}/p_{1o}) \cos k_1 x \cos k_1 y \cos\Delta_{12}, \end{aligned} \tag{30}$$

where the wavenumber $k_2 = k_1$.

III. ISOTROPIC RESTORING FORCES

The presence of gravity allows us to vary the position of a given minimum by changing the sound intensity or the chamber orientation. This, in turn, gives rise to the possibility of finding a levitation position where, by a suitable choice of the aspect ratios of the chamber, we will be able to make the restoring force constants equal. Consequently, the restoring forces will be equal (isotropic) provided the sample has a reasonably small radius.

For illustration purposes, we assume that gravity is along the z axis of the chamber. We shall examine the cylindrical case first. We will consider a rigid sphere ($f_1 = f_2 = 1$) and the modes ($0nn_z$) for simplicity. In the absence of gravity, these modes have n_z interior minimum points along the axis at positions $z/l_z = m_z/2n_z$ with $m_z = 1,3,\ldots, 2n_z - 1$. As an example, we will be concerned with the minimum at $z/l_z = 1/(2n_z)$. Since, in this case, the off-diagonal Hessian matrix terms are zero and

$$\left.\frac{\partial^2 \tilde{U}_a}{\partial \tilde{\phi}^2}\right|_{r=0} = 0, \tag{31}$$

we have that

$$\frac{1}{k_c^2}\frac{\partial^2 \tilde{U}}{\partial \tilde{z}^2}\bigg|_{r=0} = \tilde{\kappa}_z, \quad \frac{1}{k_c^2}\frac{\partial^2 \tilde{U}}{\partial \tilde{r}^2}\bigg|_{r=0} = \tilde{\kappa}_r. \tag{32}$$

Let

$$\beta = (k_z/k_r)^2 = [n_z a/(l_z \alpha_{mn})]^2, \tag{33}$$

and

$$z/l_z = k_z z/(\pi n_z). \tag{34}$$

Now, equating

$$\tilde{\kappa}_z(\beta, z/l_z) = \tilde{\kappa}_r(\beta, z/l_z), \tag{35}$$

we obtain $z/l_z = f(\beta)$, and $\tilde{\kappa}_z = \tilde{\kappa}_r = F(\beta)$. We find

$$\tilde{\kappa}_z = \tilde{\kappa}_r = \beta(2+5\beta)(17-4\beta)/[3(1+\beta)^2 \times (160\beta^2 + 84\beta + 17)], \tag{36}$$

and

$$\cos^2 k_z z = 4\beta(20\beta + 11)/(160\beta^2 + 84\beta + 17). \tag{37}$$

Thus, with β determined by the mode and chamber geometry, one can obtain the levitation position for isotropic restoring force constants and the magnitude of these constants.

In the rectangular case, as usual, we let $f_1 = f_2 = 1$ and consider the modes $(2m_x 2m_y n_z)$, where $m_x, m_y = 0,1,2,\ldots$. These modes have minima along the z axis, where the off-diagonal Hessian matrix terms are again zero. Thus we have $x/l_x = y/l_y = 0.5$, and

$$k_x x = n_x \pi (x/l_x) = 2m_x \pi (x/l_x) = m_x \pi, \tag{38a}$$

and, likewise,

$$k_y y = m_y \pi. \tag{38b}$$

We define

$$a = \left(\frac{k_z}{k_x}\right)^2 = \left(\frac{n_z}{2m_x}\right)^2 \left(\frac{l_x}{l_z}\right)^2, \tag{39a}$$

and

$$\gamma = \left(\frac{k_y}{k_x}\right)^2 = \left(\frac{m_y}{m_x}\right)^2 \left(\frac{l_x}{l_y}\right)^2. \tag{39b}$$

As in the previous case,

$$z/l_z = k_z z/(\pi n_z). \tag{40}$$

We first equate

$$\tilde{\kappa}_x(\alpha, \gamma, z/l_z) = \tilde{\kappa}_y(\alpha, \gamma, z/l_z). \tag{41}$$

This is satisfied with either $\gamma = 1$, or $\gamma = \gamma(\alpha, z/l_z)$. The case $\gamma = 1$ will not be discussed since the resultant allowable equilibrium position range is too restricted and $\tilde{\kappa}$ is extremely small. Now, let $\delta = \cos^2 k_z z$; thus we can solve for z/l_z in terms of δ and write $\gamma = \gamma(\alpha, \delta)$. We can use this last relation to eliminate γ from $\tilde{\kappa}_x$ and $\tilde{\kappa}_y$. Finally, the last condition $\tilde{\kappa}_x = \tilde{\kappa}_y = \tilde{\kappa}_z$ yields $\alpha = \alpha(\delta)$, and we have

$$\tilde{\kappa}_x = \tilde{\kappa}_y = \tilde{\kappa}_z = (5/9)\delta(1-2\delta)(5\delta+2). \tag{42}$$

IV. DISCUSSION

The lowest-order mode that can position an object within a rectangular chamber is the (221) mode.[7] This mode and its permutations (212) and (122) have 32 equilibrium positions on the chamber walls and one equilibrium position within the chamber at the center $(x/l_x = y/l_y = z/l_z = 0.5)$. In zero gravity, the sample will not move to the walls so long as it remains in the acoustic potential well surrounding the chamber center. This potential well is not isotropic, there being specific directions along which the sample can most easily move toward the walls. When a gravitational field is present, the total potential (acoustic plus gravitational) will no longer be minimum at the chamber center. Since the gravitational force will always move the sample toward a wall, the acoustic positioning force must be sufficiently large to counteract gravity. This balancing of forces is strongly dependent on the chamber orientation relative to gravity as well as on the sound-pressure level. In this section, we will explore the conditions controlling whether the sample remains levitated within the chamber or is forced to the chamber walls.

The effect of gravity on the levitation position for the (221) mode is shown in Fig. 4 for the case in which the gravitational field vector is downward along the z axis. The spatial dependence of the total potential and force is shown for three different ratios of gravity force F_g to the maximum acoustic force along the z axis F_{zo} (i.e., F_g/F_{zo}). The acous-

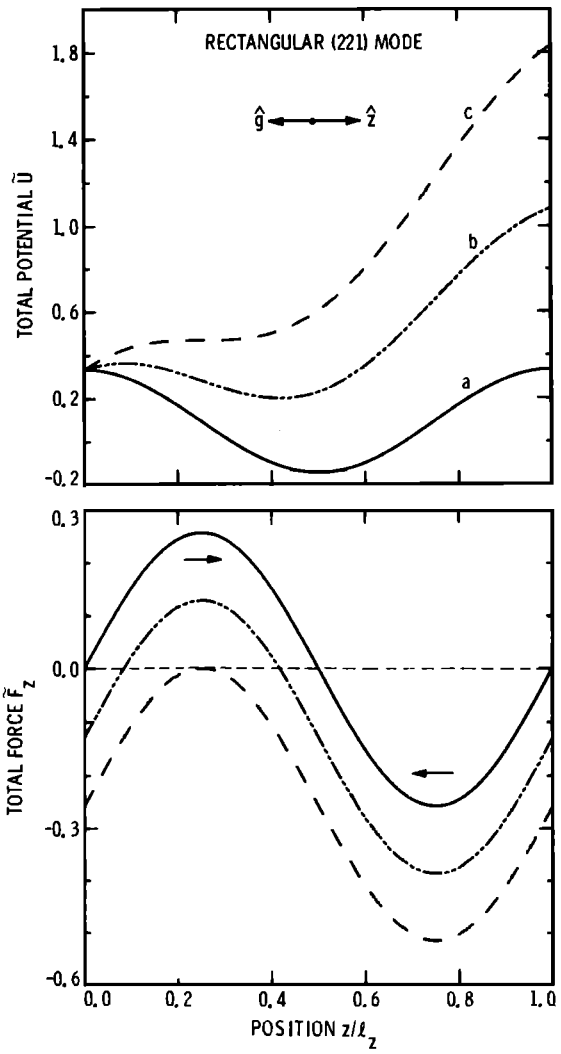

FIG. 4. Position dependence of the total potential and z force for the (221) rectangular mode in a gravitational field downward along the z axis ($\alpha = 90°, \beta = 90°, \gamma = 180°$). The three curves correspond to different ratios of the gravity force F_g to the maximum acoustic force along the z axis F_{zo}: curve a, $F_g/F_{zo} = 0$; curve b, $F_g/F_{zo} = 0.5$; curve c, $F_g/F_{zo} = 1.0$. As this ratio goes between 0 and 1, the sample equilibrium position changes between $z/l_z = 0.5$ and 0.25.

tic particle velocity associated with a given force ratio can be obtained from Eq. (6). For this chamber orientation, the maximum acoustic force is at the position $z/l_z = 0.25$. In the microgravity environment of space (or on the ground where the acoustic forces are much larger than gravity), the acoustic forces will dominate and the total potential and force profiles will be those shown by the solid curves in Fig. 4. Under these conditions, the sample is positioned at the center of the chamber where the potential is minimum and the force is zero. When the acoustic force is reduced in a ground-based laboratory so that $F_g/F_{zo} = 0.5$, the object is repositioned downward to the new minimum in the total potential as shown by the variable-dashed curve. Since the gravitational force is a constant, the total force profile is simply shifted downward by an amount equal to the gravitational force. The dashed curves correspond to the case where the maximum acoustic force F_{zo} just equals the gravity force. Now the object is metastably positioned at $(z/l_z)_{eq} = 0.25$ where the total potential has an inflection point. There will be no minimum in the total potential for any further reduction of the acoustic force (i.e., $F_g/F_{zo} > 1$) and thus under these conditions an object cannot be levitated and will fall to the bottom of the chamber.

New levitation positions within the rectangular chamber appear when the chamber, excited by the (221) mode, is now reoriented so the gravitational field vector is downward along the x axis. Figure 5 shows the spatial profile of the total potential along the x axis. Now, curve a (solid), curve b (variable dashed), and curve c (dashed) correspond to $F_g/F_{xo} = 0$, 0.5, and 1, respectively. In zero gravity

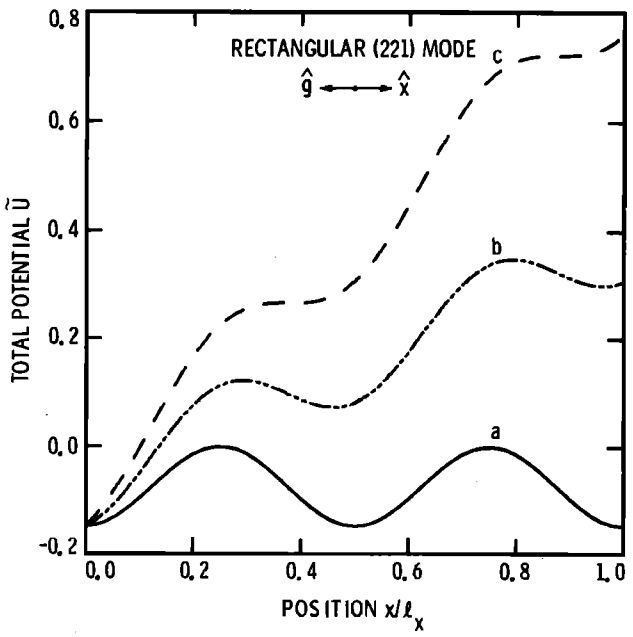

FIG. 5. The position dependence of the total potential for the (221) rectangular mode in a gravitational field downward along the x axis ($\alpha = 180°$, $\beta = 90°$, $\gamma = 90°$). For solid curve a, $F_g/F_{xo} = 0$ (zero-gravity case), the sample equilibrium positions are $(x/l_x)_{eq} = 0$, 0.5, or 1.0. For variable-dashed curve b, $F_g/F_{xo} = 0.5$ and $(x/l_x)_{eq} = 0.459$ and 0.959. For dashed curve c, $F_g/F_{xo} = 1.0$ and $(x/l_x)_{eq} = 0.375$ and 0.875. As the force ratio goes between 0 and 1, the sample equilibrium position ranges between $(x/l_x)_{eq} = 0.5$ and 0.375 or $(x/l_x)_{eq} = 1.0$ and 0.875.

($F_g/F_{xo} = 0$), there are potential minima at the x walls given by $x/l_x = 0$, 1 in addition to the minimum at the midplane $x/l_x = 0.5$. When the gravitational force becomes comparable to the acoustic force, as in the variable-dashed curve, the potential minima are again shifted to lower positions leading now to two levitation positions within the chamber. As the gravitational force becomes equal to the acoustic force, the potential curve develops two inflection points (metastable levitation positions) at $x/l_x = 0.375$ and 0.875, as shown by the dashed curve.

A simple analytic expression for the equilibrium levitation position for the (221) mode is obtained when gravity is directed along a principal axis of the rectangular chamber. For this case, the balancing of acoustic and gravitational forces requires

$$F_g = F_{ai} = F_{io} \sin k_i x_i, \tag{43}$$

where F_{io} is the maximum acoustic force that occurs at positions satisfying $\sin k_i x_i = 1$ and $k_i = \pi n_i / l_i$. Using Eqs. (7) and (43), we find

$$F_g/F_{io} = \tilde{F}_g/\tilde{F}_{io} \tag{44}$$

under equilibrium conditions. Now, solving Eq. (43) for the equilibrium position x_i/l_i yields

$$\frac{x_i}{l_i} = \frac{1}{2}\left[1 - \frac{1}{\pi n_i}\tan^{-1}\left(\frac{\tilde{F}_g}{\tilde{F}_{io}}\right)\right]. \tag{45}$$

The normalized gravitational force $\tilde{F}_g$ can be obtained from Eq. (7) and

$$\tilde{F}_{io} = \left(\frac{f_2}{2}\right)\left(\frac{k_i}{k}\right)\left(\frac{k_z}{k}\right)^2, \quad \text{for } i = x \text{ or } y \tag{46a}$$

and

$$\tilde{F}_{io} = \left(\frac{k_i}{k}\right)\left[\frac{f_1}{3} + \left(\frac{f_2}{2}\right)\left(\frac{k_z}{k}\right)^2\right], \quad \text{for } i = z. \tag{46b}$$

Let us now discuss the levitation capabilities of a rectangular chamber that is gradually being reoriented relative to gravity. For example, consider a chamber initially oriented with the gravitational field downward along the z axis ($\alpha = 90°, \beta = 90°, \gamma = 180°$) and excited in the (221) mode at a fixed sound-pressure level (SPL). The chamber is then slowly rotated about the y axis by varying the angle α until the gravitational field is finally oriented along the x axis ($\alpha = 180°$, $\beta = 90°$, $\gamma = 90°$). As the chamber orientation varies, the y coordinate of the equilibrium position will remain constant at $y/ly = 0.5$. Figure 6 shows the x and z equilibrium coordinates as the orienting angle α is varied from 90° to 180° for three SPLs. The sample will remain levitated throughout the reorientation for sufficiently large SPLs (curve a, $F_g/F_{xo} = 0.5$), while, for sufficiently low SPLs (curve c, $F_g/F_{xo} = 1$), the sample will fall for a range of α values indicated by the vertical arrows. As $F_g/F_{xo} \to 1$, the sample will gradually deviate further from the chamber center during the reorientation process. The minimum SPL to just remain levitated throughout the orientation range approximately corresponds to $F_g/F_{xo} = 0.98$. The chamber orientation corresponding to the weakest levitation position is at $\alpha \simeq 165°$.

When a rectangular chamber is oriented with the direc-

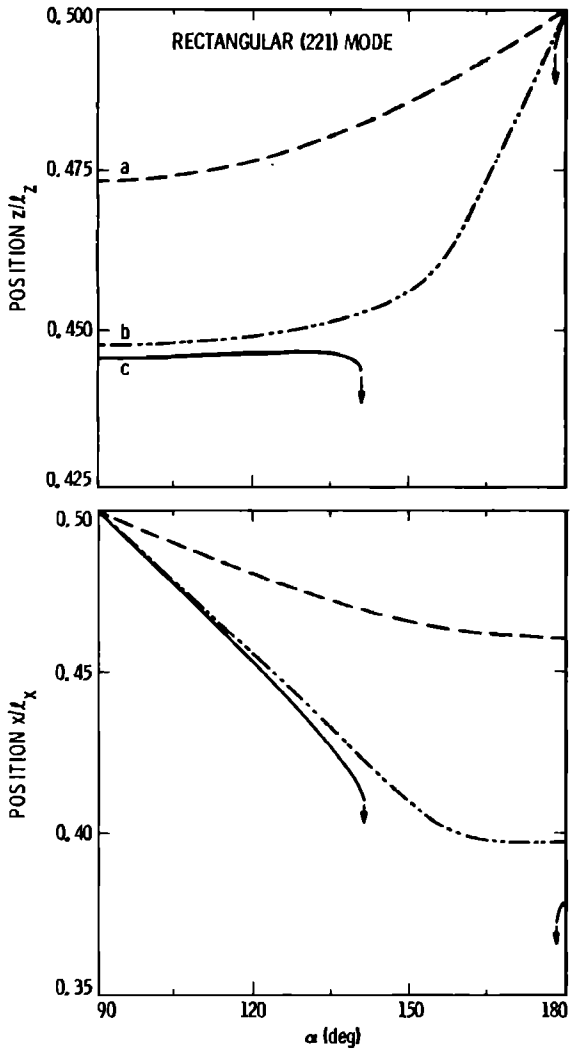

FIG. 6. Equilibrium position as a function of chamber orientation about the y axis for the (221) rectangular mode. For this case $\beta = 90°$, $\gamma = 270° - \alpha$, and $y/l_y = 0.5$. A gravitational field along the z or x axis corresponds to $\alpha = 90°$ and 180°, respectively. The curves correspond to fixed acoustic sound-pressure levels equivalent to the arbitrarily chosen force ratios: curve a, $F_g/F_{xo} = 0.5$; curve b, $F_g/F_{xo} = 0.965$; curve c, $F_g/F_{xo} = 1.0$. For larger force ratios (low SPL), there are orientation ranges where the acoustic force is insufficient to overcome gravity and the sample falls (see arrows).

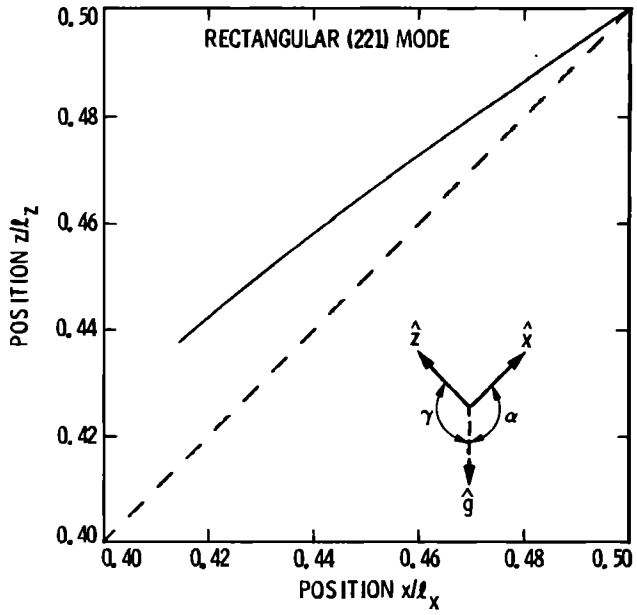

FIG. 7. Equilibrium range for the (221) rectangular mode in a chamber oriented between the z and x axes ($\alpha = 135°$, $\beta = 90°$, $\gamma = 135°$). The solid curve is allowable levitation range. The dashed line is the direction of gravity. In the earth's gravitational field, the sample is never positioned along the gravity field direction.

tion of gravity along a major axis (x, y, or z), the allowable sample levitation range is on the major axis (i.e., along the direction of gravity). This situation was illustrated in connection with Figs. 4 and 5. However, in general, for an arbitrarily oriented chamber, the sample equilibrium position will not lie along the direction of gravity. An example of this case is shown in Fig. 7 for the same chamber discussed in Fig. 6, but oriented at $\alpha = 135°$. The solid curve defines the allowable range of equilibrium positions (x/l_x,z/l_z). The dashed line defines the direction of gravity. For zero gravity conditions ($F_g/F_{ai} = 0$), the equilibrium position is at the chamber center ($x/l_x = 0.5$, $z/l_z = 0.5$). As the force ratio is increased, the equilibrium position moves below the center and gradually deviates from the direction of gravity until levitation can no longer be maintained.

This phenomenon can be understood from a consideration of the forces on a sample that *is* along the gravity direction. In general, for an arbitrary chamber orientation, this sample will experience some acoustic force components that are not along the gravity direction. The sample will move off the gravity direction until it reaches a position where all the total force components become zero.

In practical experimental levitation studies, a sample is generally released from a position that is not necessarily the ultimate equilibrium position. The sample will then follow a trajectory to the nearest equilibrium position that depends on the mode of excitation, starting position, and the ratio of the gravitational to acoustic forces. We have developed computer programs to determine the equilibrium trajectory for rectangular and cylindrical levitators. Figure 8 shows the equilibrium trajectory for a sample released at position $x/l_x = y/l_y = 0.4$, and $z/l_z = 0.5$ in a rectangular chamber excited in the (221) mode, the lowest-order mode to position a sample within the chamber. The various curves represent different SPLs (force ratios) for the chamber oriented with gravity downward along the z axis. Since there is no gravitational force component along the x or y directions, the sample trajectory along these directions is unaffected by varying the SPL (force ratio), and the final x, y equilibrium coordinates will always be $x/l_x = y/l_y = 0.5$. However, the trajectory and final equilibrium position along the z direction is strongly dependent on the SPL. In the zero-gravity case, the z coordinate will remain unchanged at $z/l_z = 0.5$ (curve a). As the SPL decreases (increasing force ratio), the z coordinate of the trajectory initially decreases beyond its final equilibrium z position before homing into this final value. For SPLs below a cutoff value corresponding to $F_g/F_{zo} = 0.57$, the sample will be unable to remain levitated and it will fall to the nearest equilibrium position for this mode at the bottom of the chamber.

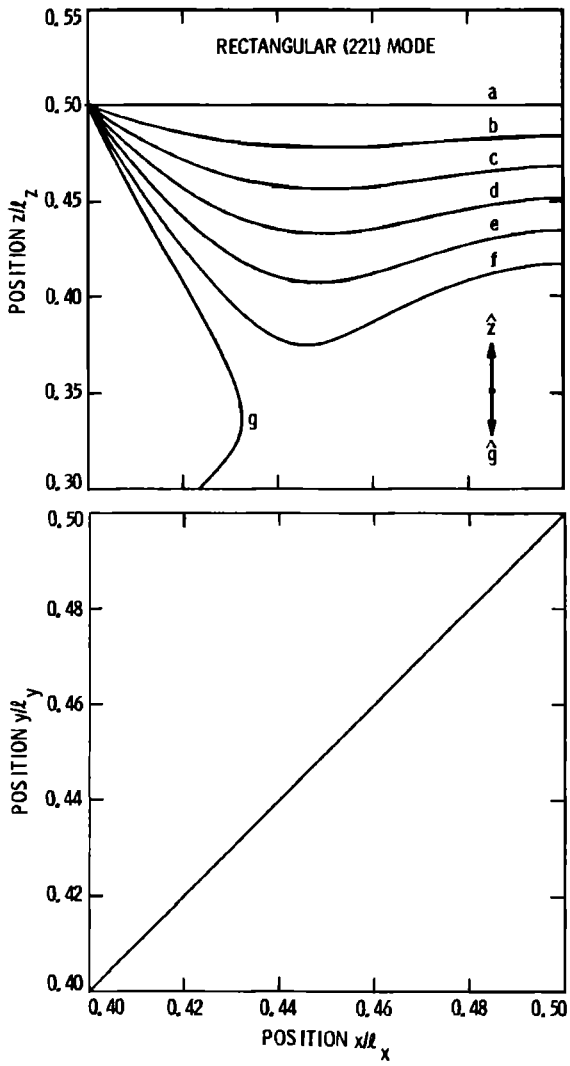

FIG. 8. Equilibrium trajectory for (221) rectangular mode with gravitational field downward along the z axis ($\alpha = 90°, \beta = 90°, \gamma = 180°$). Initial sample position: $x/l_x = y/l_y = 0.4$, $z/l_z = 0.5$. Final sample equilibrium position ($x/l_x = y/l_y = 0.5$ and z/l_z determined by force ratios): a, $F_g/F_{zo} = 0$; b, 0.1; c, 0.2; d, 0.3; e, 0.4; f, 0.5; and g, 0.6. For $F_g/F_{zo} = 0.6$, the acoustic force was unable to overcome gravity and the sample fell to the bottom of the chamber.

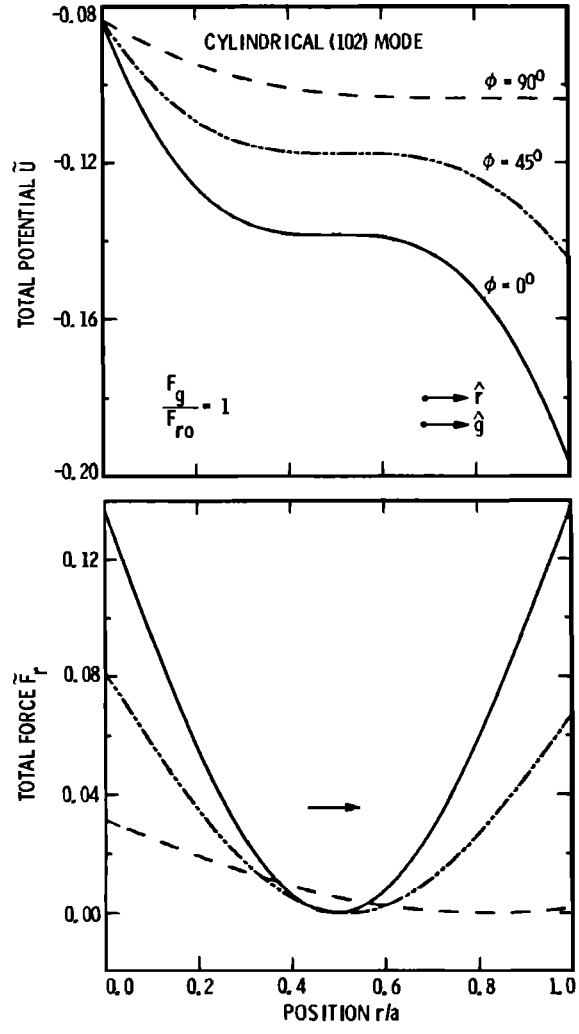

FIG. 9. Position dependence of the total potential and radial force for the (102) cylindrical mode. The equilibrium position in zero gravity, $F_g/F_{ro} = 0$, is at the chamber center $r/a = 0$, $z/l_z = 0.5$. These curves correspond to $F_g/F_{ro} = 1$ for the gravitational field along the directions $\phi = 0$, 45°, and 90°. The inflection point in the total potential determines the maximum equilibrium position for each orientation; i.e., $(r/a)_{max} = 0.493$, 0.516, and 0.808 for $\phi = 0$, 45°, and 90°, respectively.

For cylindrical geometry, the x and y axes are transformed into r and ϕ axes. An important levitation mode in a cylindrical chamber is the (102) mode, which positions an object at the chamber center ($r/a = 0$, $z/l_z = 0.5$) in zero gravity. To illustrate the effects of gravity in this geometry, we show in Fig. 9 the total potential and radial force for the (102) mode with the gravitational field along the radial direction for $\phi = 0$, 45°, and 90°. In each case, the curves correspond to the minimum acoustic force necessary to just levitate the object (i.e., $F_g/F_{ro} = 1$). The inflection point for each total potential curve corresponds to the maximum radial equilibrium position along that ϕ direction. These equilibrium positions correspond to $(r/a)_{max} = 0.493$, 0.516, and 0.808 for $\phi = 0$, 45°, and 90°, respectively. As the acoustic force is gradually increased above its minimum value, the equilibrium position will gradually approach the zero-gravity value, $r/a = 0$. The radial force curves show that the restoring force is maximum for $\phi = 0$ and is gradually reduced as ϕ approaches 90°, where it is asymmetric and very weak.

It is clear from this figure that, as the cylindrical chamber is reoriented relative to gravity by rotation about the z axis, a minimum levitation surface will be generated. This surface will not be a circle since $(r/a)_{max}$ varies with ϕ. The actual shape of this surface can be determined from the maximum radial force and position as a function of ϕ, as shown in Fig. 10.

If the cylinder were oriented with the gravitational field downward along the z axis, the allowable levitation range is $0.25 \leqslant z/l_z \leqslant 0.5$. For this orientation, the equilibrium position and maximum acoustic force F_{zo} can be determined from Eqs. (44) and (46) with $x_i = z$. If the cylinder were now turned 180° so the positive z axis is downward along the gravitational direction, the allowable levitation range would be $0.5 \leqslant z/l_z \leqslant 0.75$. We can carry this idea one step further and obtain the position of the maximum acoustic restoring

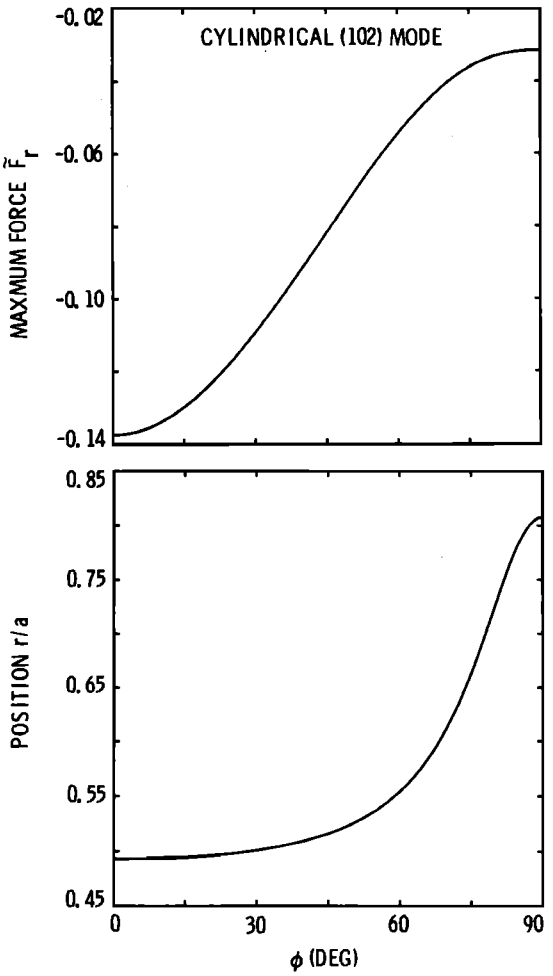

FIG. 10. Maximum acoustic force F_r and position r/a as a function of ϕ in midplane $z/l_z = 0.5$ for (102) cylindrical mode. The position of the maximum acoustic restoring force, along all chamber orientations, determines the contour of the allowable equilibrium levitation volume in the presence of gravity.

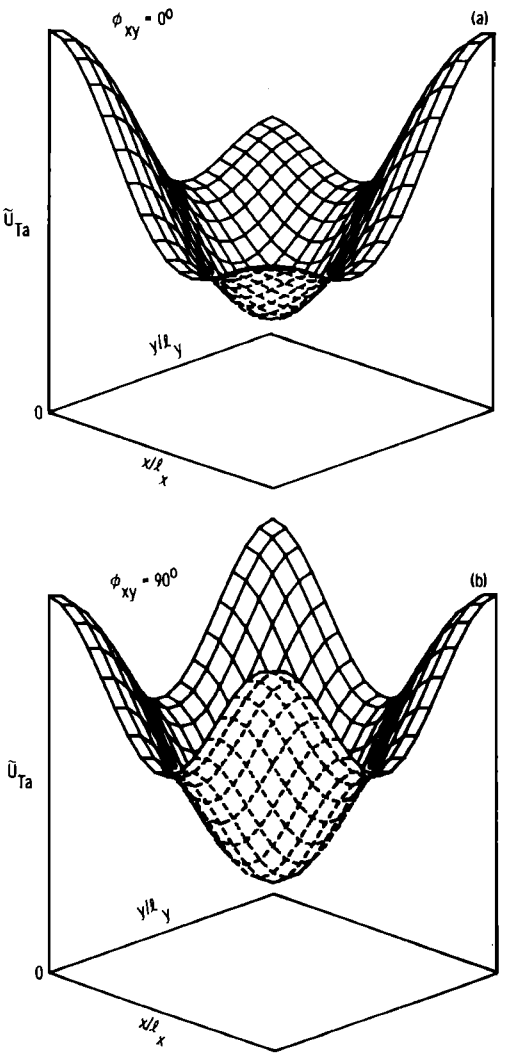

FIG. 11. Hidden line plots of the total acoustic potential for the ACES triple-axis levitator for the case of zero gravity. This plot corresponds to the plane $z/l_z = 0.5$. (a) $\phi_{xy} = 0°$ nonrotation case. (b) $\phi_{xy} = 90°$ maximum rotation case. The $\phi_{xy} = 90°$ case has fourfold symmetry while the $\phi_{xy} = 0°$ case has only twofold symmetry with the steepest potential wells along the diagonals.

force along all chamber orientations θ and ϕ, which could then be used to determine a volume of possible equilibrium levitation points for the (102) mode in a gravitational field. This process can be used for any levitation mode in any geometry to determine the size of the levitation volume in gravity, which is in contrast to a unique levitation point in zero gravity.

When more than one acoustic mode is used to levitate an object, the total acoustic potential can be determined by the superposition of the individual potentials associated with each excited mode as presented in Sec. II. An important example of this concept is the triple-axis levitator that requires the excitation of three orthogonal plane-wave modes in a rectangular chamber.[1] These modes position an object at the center of the chamber. This design concept was used in the acoustic containerless experimental system (ACES) that was flown on the Space Shuttle.[13] The ACES chamber had a square cross section that led to a degeneracy in the x and y plane-wave modes. Thus the ACES chamber is an example of the mixed case discussed in Sec. II. This degeneracy allowed both modes to be excited by a common oscillator and to have a relative phase difference. This phase difference was shown to produce torques on the levitated sample that lead to rotation about the z axis.[11] No torque is produced with a phase difference of 0° or 180°.

It is of interest to understand the effects of a phase difference on the total potential and thus on the translational stability of the rotating or nonrotating sample in a zero gravity or ground-based environment. The hidden line plots of the total potential in Fig. 11 illustrate the effects of the phase difference between the degenerate modes of the ACES triple-axis levitator in a zero-gravity environment on the plane $z/l_z = 0.5$. The ACES levitator had chamber aspect ratios of $l_x/l_y = 1$ and $l_x/l_z = 0.91$. Figure 11(a) and 11(b) shows the total potential for phase difference $\phi_{xy} = 0°$, and 90°, respectively, for equal sound-pressure levels for each mode. At 0° phase difference (nonrotation case), the total potential minimum at the center of the chamber is asymmetric, which implies that the acoustic force field on the sample is anisotropic. At 90° phase difference (rotation case), the total po-

tential becomes more symmetric and thus the acoustic forces become stronger and more isotropic. It is interesting to note that the shape of the total potential in the $z/l_z = 0.5$ plane for the nondegenerate case ($l_x \neq l_y \neq l_z$) is equivalent to the mixed case ($l_x = l_y \neq l_z$) with the phase difference of 90° shown in Fig. 11(b).

Figure 12 shows hidden line plots of the total potential on the plane $z/l_z = 0.5$ for the ACES triple-axis levitator oriented with the x axis along the 1-g gravitational field and with each mode excited at the same sound-pressure level. Figure 12(a) and (b) corresponds to phase differences $\phi_{xy} = 0°$ and 90°, respectively, for the case of the minimum acoustic force needed to just levitate the sample ($F_g/F_{xo} = 1$). For this condition, the minimum in the total potential in this plane occurs at $x/l_x = 0.25$, and $y/l_y = 0.5$. Again, at 90° phase difference (rotation case), the total potential near the minimum becomes steeper and more symmetric than the 0° phase difference case.

As more powerful acoustic drivers are developed, acoustic levitators are being used more for containerless processing studies in ground-based laboratories. For many containerless experiments, it will be important to control the acoustic force anisotropy that can affect the shape of a liquid sample.[14] In Sec. III, we determined some experimental conditions needed to obtain an isotropic force field at the position of the levitated sample. We have applied these conditions to the case of a cylindrical chamber oriented with the z axis along gravity and excited in the (011) mode. For this orientation, the levitation range for the (011) mode is $0.25 \leqslant z/l_z \leqslant 0.5$. In Fig. 13, we show the sample equilibrium position dependence on chamber aspect ratio a/l_z and restoring force constant κ for an isotropic total force field. The normalized isotropic force constant is zero at the end points of the levitation range and reaches a maximum of 0.093 at position $z/l_z = 0.28$ where the required aspect ratio is $a/l_z = 0.776$.

We have also applied the isotropic force field conditions to a (221) mode in a rectangular chamber where the z axis was along the gravitational direction. The levitation range of the (221) mode for this orientation is $0.25 \leqslant z/l_z \leqslant 0.5$. The requirements for force isotropy are shown in Fig. 14 for the chamber aspect ratios l_x/l_y and l_x/l_z and the normalized isotropic force constant. The rectangular (221) mode and the

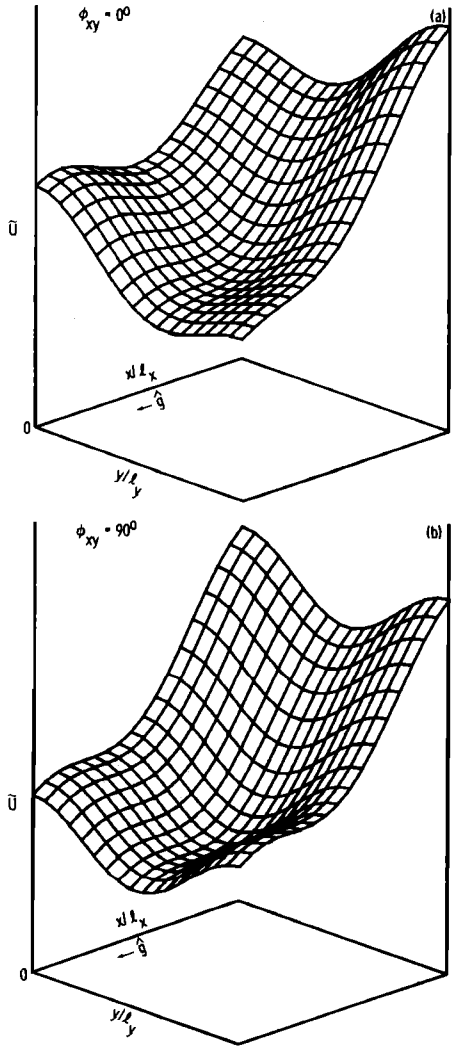

FIG. 12. Hidden line plots of the total potential in the levitation plane $z/l_z = 0.5$ for the ACES triple-axis levitator oriented with gravity downward along the x axis. These surfaces are for the minimum acoustic force needed to just levitate the sample ($F_g/F_{xo} = 1$). (a) $\phi_{xy} = 0°$ nonrotation case. (b) $\phi_{xy} = 90°$ maximum rotation case.

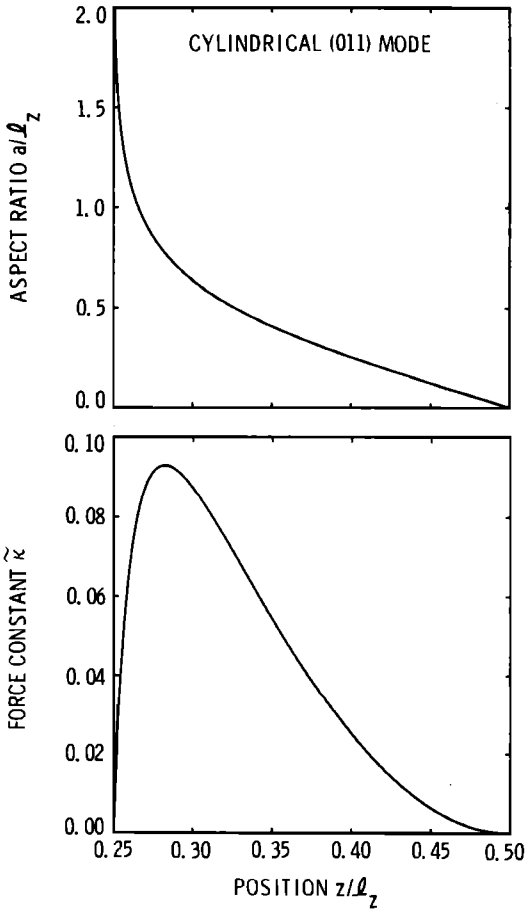

FIG. 13. Position dependence of the chamber aspect ratio and restoring force constant for an isotropic total force field in the cylindrical (011) mode. The maximum isotropic restoring force constant occurs at $z/l_z = 0.282$ for an aspect ratio $a/l_z = 0.776$.

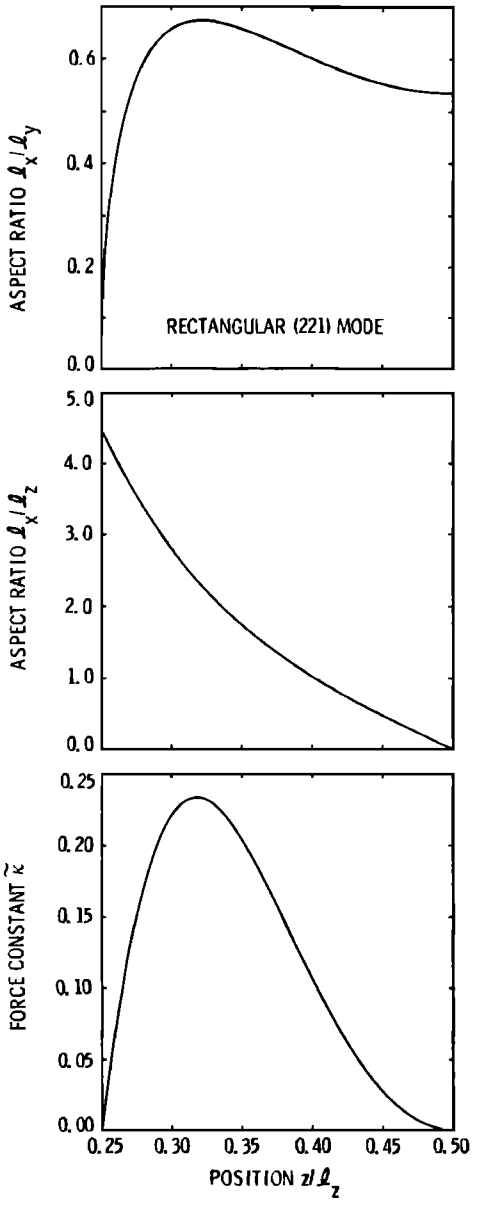

FIG. 14. Position dependence of the chamber aspect ratios and restoring force constant for an isotropic total force field in the (221) rectangular mode. The maximum isotropic restoring force constant occurs at $z/l_z = 0.321$ for $l_x/l_y = 0.673$ and $l_x/l_z = 2.36$.

cylindrical (011) mode have similar acoustic levitation properties as can be seen by comparing the dependence of the equilibrium position for l_x/l_z and κ in Fig. 14 to a/l_z and κ in Fig. 13. In the case of the (221) rectangular mode, the normalized isotropic force constant reaches a maximum of 0.23, where the required chamber aspect ratios are $l_x/l_y = 0.673$ and $l_x/l_z = 2.36$.

V. CONCLUSION

In conclusion, we have developed general expressions for acoustic levitation in the presence of a gravitational field for arbitrarily oriented rectangular, spherical, and cylindrical chambers. Examples of the effects of gravity were presented for levitation modes in rectangular and cylindrical chambers with particular emphasis on the triple-axis levitator concept used in the design of the ACES space module. For arbitrarily oriented chambers, the presence of gravity leads to sample positioning within a "levitation" volume that surrounds the unique sample position associated with acoustic forces only. The sample position within this levitation volume is determined by the chamber orientation and the ratio of the gravitational to acoustic force. The ability to vary the position of the levitated sample provides a method for adjusting the total force field anisotropy and thus the sample shape. We have determined the experimental conditions required for obtaining an isotropic total force field at the position of a small levitated sample for the (221) rectangular and (011) cylindrical levitation modes.

The approach used in this paper of summing the acoustic and gravitational potentials to obtain the total potential can also be applied to other fields having a potential. The extension of the present work to include the simultaneous excitation of acoustic and electrostatic or acoustic and electromagnetic force fields may lead to interesting hybrid positioning techniques for use in future microgravity materials processing programs.

ACKNOWLEDGMENTS

We thank Dr. H. W. Jackson for reviewing the manuscript, G. Aveni for technical support, and A. Belcastro for excellent secretarial support in typing this manuscript. The research described in this paper was carried out by the Jet Propulsion Laboratory, California Institute of Technology, under contract with the National Aeronautics and Space Administration.

[1] M. Barmatz, "Overview of containerless processing technologies," in *Proceedings of the Symposium on Materials Processing in the Reduced Gravity Environment of Space*, Boston, MA (Elsevier, New York, 1982), p. 25.
[2] T. G. Wang, E. Trinh, W-K. Rhim, D. Kerrisk, M. Barmatz, and D. D. Elleman, "Containerless processing technologies at the Jet Propulsion Laboratory," ACTA Astronautica, J. Int. Astronautics **11**, 233 (1984).
[3] L. V. King, "On the acoustic radiation pressure on spheres," Proc. R. Soc. London Ser. A **147**, 212 (1934).
[4] K. Yosioka and Y. Kawasima, "Acoustic radiation pressure on a compressible sphere," Acoustica **5**, 167 (1955).
[5] L. A. Crum, "Acoustic force on a liquid droplet in an acoustic stationary wave," J. Acoust. Soc. Am. **50**, 157 (1971) and "The acoustic radiation pressure on a liquid droplet in a stationary sound field," Michelson Phys. Lab., U.S. Naval Academy, Tech. Rep. No. C-1 (1970).
[6] M. A. H. Weiser and R. E. Apfel, "Extension of acoustic levitation to include the study of micron-size particles in a more compressible host liquid," J. Acoust, Soc. Am. **71**, 1261 (1982).
[7] M. Barmatz and P. Collas, "Acoustic radiation potential on a sphere in plane, cylindrical, and spherical standing wave fields," J. Acoust. Soc. Am. **77**, 928 (1985).
[8] L. P. Gor'kov, "On the forces acting on a small particle in an acoustic field in an ideal fluid," Sov. Phys. Dokl. **6**, 773 (1962); translated from Dokl. Akad. Nauk SSSR **140**, 88 (1961).
[9] P. Collas and M. Barmatz, "Acoustic radiation force on a particle in a temperature gradient," J. Acoust. Soc. Am. **81**, 1327 (1987).
[10] T. G. Wang, M. M. Saffren, and D. D. Elleman, "Acoustic chamber for weightless positioning," AIAA paper No. 74-155 (1974).
[11] F. G. Busse and T. G. Wang, "Torque generated by orthogonal acoustic waves—Theory," J. Acoust. Soc. Am. **69**, 1634 (1981).
[12] Our definition of v_0 is the same as in Ref. 7, although there we referred to it as the maximum particle velocity; this latter statement applies only to rectangular geometry.
[13] The ACES module was flown on the Space Shuttle flight STS-41B, January 1984.
[14] H. W. Jackson, M. Barmatz, and C. Shipley, "Equilibrium shape and location of a liquid drop acoustically positioned in a resonant rectangular chamber," J. Acoust. Soc. Am. **84**, 1845 (1988).